*International Conference on Mechanical, Industrial and Materials Engineering 2013 (ICMIME2013)*
*1-3 November, 2013, RUET, Rajshahi, Bangladesh.*

***Paper ID: ABS_037_ME***

# Flow over Circular Cylinders in Axial Flow with Different Nose Shapes

Qin Sun, Md. Mahbub Alam*, C.W. Wong and Y. Zhou

Institute for Turbulence-Noise-Vibration Interaction and Control, Shenzhen Graduate School, Harbin Institute of Technology, Shenzhen, China
*email: alamm28@yahoo.com; alam@hitsz.edu.cn

## Abstract

*Wall pressure measurements were performed in the separation bubble and behind the shear-layer reattachment on a blunt circular cylinder in axial flow, with Reynolds number ranging from $3.3\times10^3$ to $5\times10^4$ based on the cylinder diameter and free-stream velocity. In addition, the effects of nose shape as well as yaw angle on the flow features were investigated with conical and hemispherical noses. Time-mean pressure coefficient $C_p$, fluctuating (rms) pressure coefficient $C_P'$, and power spectral density function of fluctuating pressure are presented . It was found that $C_p$ and $C_P'$ are highly sensitive to $Re_D$ for the hemispherical nose. The blunt nose presents highest $C_P'$, while the hemispherical nose corresponds to the lowest $C_P'$. With increasing yaw angle from 0° to 3.5°, $C_p$ declines and $C_P'$ increases for both the blunt and conical cases, while those for hemispherical case vary less regularly.*

Keywords: Separation, Axial and near- axial flow, Wall pressure, Nose shape.

## 1. Introduction

The typical configuration where flow separation and reattachment occur on the leading edge of a circular cylinder in axial flow is common in engineering field, such as aircraft fuselages, submarines, missiles, road vehicles, etc. The separation and reattachment of the flow lead to a formation of bubble/cavitation that is a major source of disturbance, vibration, and noise.

A number of works on the features of flow over a blunt cylinder have been done in the literature (e.g. [1-6]). The reattachment length $x_R/D$ is a crucial parameter to characterize the flow near the leading edge. See Fig. 1 for the definition of $x_R$ and $D$ (cylinder diameter). The $x_R/D$ dramatically decreases from 2.4 to 1.5 when the Reynolds number ($Re_D$) based on $D$ varies from $2\times10^3$ to $10^4$. Beyond $Re_D = 10^4$, $x_R/D$ is about 1.5 ~ 1.6, independent of $Re_D$. Ota & Mogegi [7] measured the turbulent characteristics using hotwire at $Re_D = 4.21\times10^4$ and observed that the turbulent boundary layer becomes fully developed at least a distance of $10D$ from the leading edge. Kiya et al. [2] measured the surface pressure fluctuation at $Re_D = 2\times10^5$ along the reattachment line with a number of pressure taps. They observed that the flow in the separation bubble oscillates at two different frequencies. While the low frequency was connected to the flapping motion of the separated shear layer, and the other was associated with the shedding of the large-scale vortices from the separated zone.

Though the front part (nose) of the body in engineering applications is not always blunt, but may be of the cone or hemispherical shape, fluid dynamics around a cylinder with a cone or hemispherical nose has received much less attention than that around a blunt cylinder. Tayler et al. [8] estimated the shedding frequencies of circular cylinders of cone-shaped nose and hemispherical nose from the power spectral density functions of sectional lift coefficients obtained by integrating the pressure data measured at 24 pressure taps at the mid-span of the model. They found that variation in normalized shedding frequency with $Re_D$ from $1\times10^4$ to $3\times10^4$ was not significant in both cases.

Researches on features of flow near the leading edge of the blunt cylinder were conducted at some particular $Re_D$, while $Re_D$ effects on the surface pressure fluctuation in the flow separation region is not yet well understood for not only blunt nose, but also cone-shaped and hemispherical noses. In addition, the incident flow on the cylinder-like submarines in reality is always not axial, but may at a small yaw angle. The effect of yaw angle on the leading edge flow behavior is however not well understood. In fact, the pressure fluctuation at a

point is the integrated effect of the velocity fluctuation, hence giving an overall picture of the flow around the point. In the present paper, the surface pressure fluctuation in the separation of circular cylinders with blunt, conical, hemispherical noses were investigated experimentally, with $Re_D$ ranging from $3.3\times10^3$ to $5\times10^4$. Apart from a cylinder in axial flow, the cylinder with yaw angle of 2° and 3.5° was studied, as well. Time-mean and rms pressures are measured at points immediately behind the shear-layer separation, ahead the reattachment and following the reattachment (Fig. 1a) and $Re_D$ effects are discussed. FFT analysis of fluctuating pressures is also done to extract frequencies of shear-layer flapping and large-scale vortices.

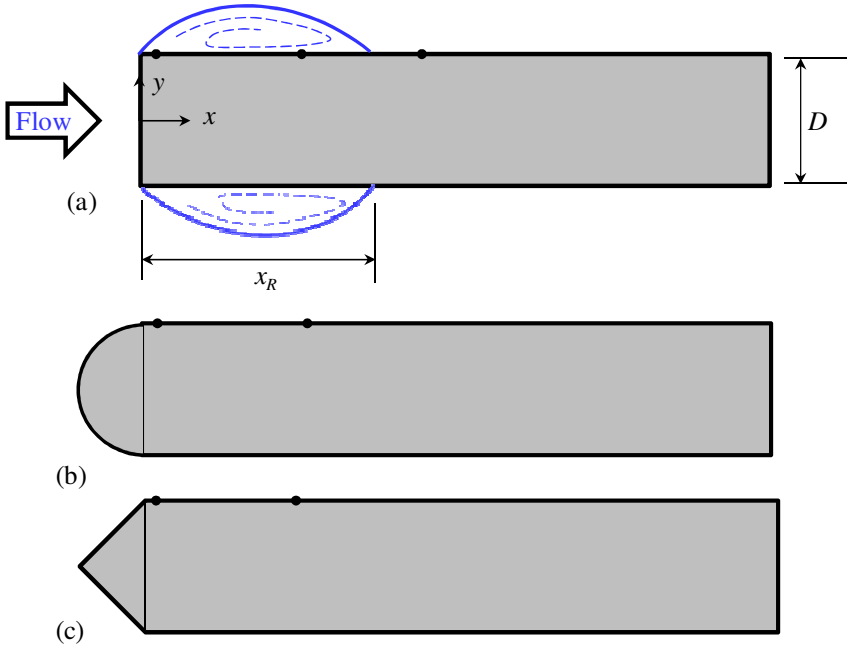


**Fig. 1.** Sketches of models. (a) Blunt cylinder and definition of reattachment length $x_R$, (b) hemispherical-nose cylinder, (c) cone-nose cylinder. Small solid circles denote the pressure tap positions.

## 2. Experimental approach

Experiments were performed in a closed-circuit wind tunnel with a 3-m-long test section of 0.9 m in width and 1.0 m in height. The flow non-uniformity was within ± 0.1% (rms) within the central cross sectional area of 0.85 m × 0.95 m in the test section, and the longitudinal turbulence intensity was less than 0.2% in the absence of the cylinder. The free-stream velocity, $U_\infty$, was varied from 6.65 to 46.8 m/s. Two different cylinders of $D$ = 7.5 and 16 , each having an aspect ratio of 12, were adopted to extend $Re_D$ range from $3.3\times10^3$ to $5\times10^4$. Furthermore, the cylinder with $D$ = 16 mm was adopted with three noses, i.e., blunt, conical and hemispherical. The model was positioned horizontally at the centerline of the test section and supported by a L-shape stainless steel rod which was vertically fixed by a metal stand without being in contact with the wind tunnel wall, so that the model vibration caused by the wind tunnel can be avoided. Two yaw angles of α = 2° and 3.5° are achieved through rotating a plate which holds the L-shape support.

It is known that $x_R/D$ is larger than 1.5 at least over a wide range of $Re_D$ as mentioned in the introduction. We were interested to know the difference in pressure fluctuations (i) immediately behind the separation, (ii) around the center of the separation bubble and (iii) behind the reattachment. Therefore three pressure taps on the cylinder of $D$ = 7.5 mm at $x/D$ = 0.15, 1.0 and 2.5, respectively were made (Fig. 1). The cylinders of $D$ = 16 mm were however furnished with two pressure taps only at $x/D$ = 0.15 and 1.0, respectively. Therefore, data for $x/D$ = 2.5 will be available at $Re_D < 2.5\times10^4$ only. All the pressure taps were connected to a pressure transducer (Toyoda PD104K) with a small cavity between the pressure taps and the transducer diaphragm. The transducer had an excellent frequency response up to 450 Hz. For yaw angle cases, the pressure taps were on the downstream side.

## 3. Results and discussion

Figure 2 shows time-mean surface-pressure coefficient $C_P = (P - P_\infty)/(0.5\rho U_\infty^2)$ and fluctuating (rms) pressure coefficient $C_P^{'}$ at $x/D$ = 0.15, 1.0 and 2.5 for the blunt cylinder, where $P$ is the pressure on the cylinder surface, $P_\infty$ is pressure in free-stream flow and $\rho$ is the density of air. The figure also includes data from the literature, showing validation of the present measurements. At $Re_D$ = $3.3\times10^3$ ~ $1.0\times10^4$, $C_p$ and $C_P^{'}$ at $x/D$ = 1.0 decline and increase, respectively, which is attributed to the fact that the reattachment of the separated shear layer proceeds towards the leading edge with $Re_D$ which enhances the turbulence in the bubble. On the other hand, for $Re_D > 1.0\times10^4$, both $C_p$ and $C_P^{'}$ tend to be constant as a result of the bubble size being almost insensitive to $Re_D$. However, the $C_p$ and $C_P^{'}$ at $x/D$ = 0.15 augment slightly, because the shear layer near the separation narrows when $Re_D$ is increased. While $C_p$ at $x/D$ = 0.15 and 1.0 ranges between -0.52 and -0.68, that at $x/D$ = 2.5 is between -0.1 and 0.0. The observation implies that $C_p$ magnitude in the cavity is larger than that behind the reattachment. Ota's [1] data measured at $x/D \approx 0.15$ and 2.3 ($Re_D = 6.62\times10^4$) and Kiya et al.'s [2] data at $x/D \approx 0.8$ ($Re_D = 10^5$), both accord well with our present measurements, according to the trends of $C_p$. With an increase in $Re_D$, $C_P^{'}$ at $x/D$ = 2.5 wanes rapidly. The waning of $C_P^{'}$ results from the combine effect of shifts of both shear-layer transition and reattachment to the upstream.

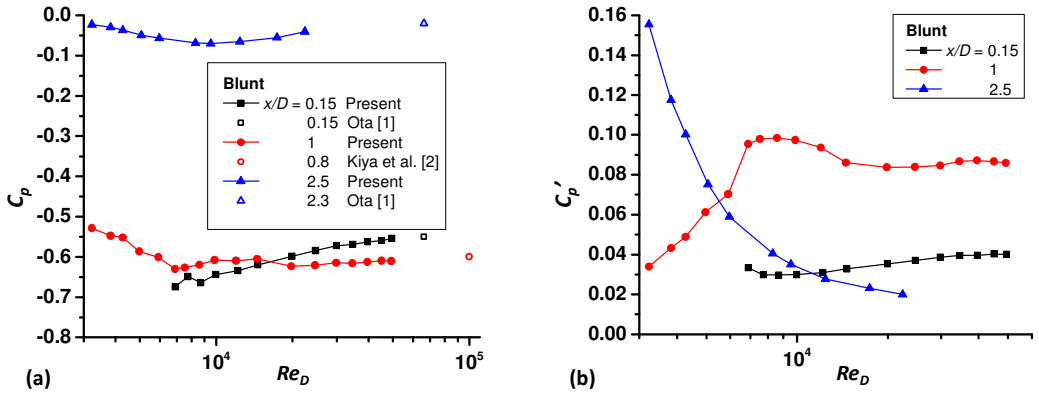


**Fig. 2.** Dependences on $Re_D$ of (a) time-mean pressure coefficient $C_p$, and (b) fluctuating pressure coefficient $C_P^{'}$.

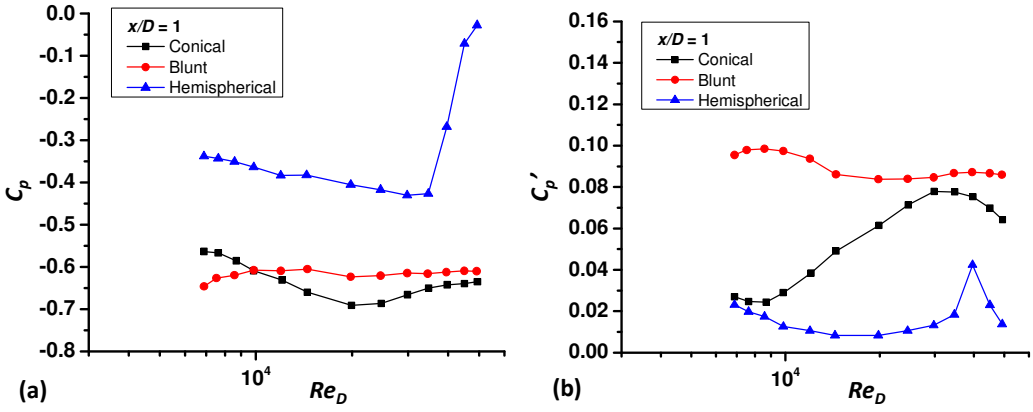


**Fig. 3.** Dependences on $Re_D$ for the three nose shapes of (a) time-mean pressure coefficient $C_p$, and (b) fluctuating pressure coefficient $C_P^{'}$.

Figure 3 compares $C_p$ and $C_P^{'}$ at $x/D$ = 1.0 between the three nose shapes. The magnitude of $C_p$ is smaller for the hemispherical nose and larger for the conical nose, compared to that for the blunt nose. Furthermore $C_p$ and $C_P^{'}$ are highly sensitive to $Re_D$ for the hemispherical nose, due to easy shift of the separation point with increasing $Re_D$. The blunt nose presents the highest $C_P^{'}$, while the hemispherical nose corresponds to the lowest $C_P^{'}$. For hemispherical nose, a sharp peak in $C_P^{'}$ variation at $Re_D$ = 5×10$^4$ is observed and $C_p$ around the same $Re_D$ recovers drastically, Both observations indicate that the reattachment occurs beyond and before $x/D$ = 1.0 for $Re_D$ < 5×10$^4$ and $Re_D$ > 5×10$^4$, respectively, and exactly at $x/D$ = 1.0 at $Re_D$ = 5×10$^4$. On the other hand, for the blunt and conical noses, absences of recovery in $C_p$ and sharp peak in $C_P^{'}$ suggest that the reattachment nestles beyond $x/D$ = 1.0.

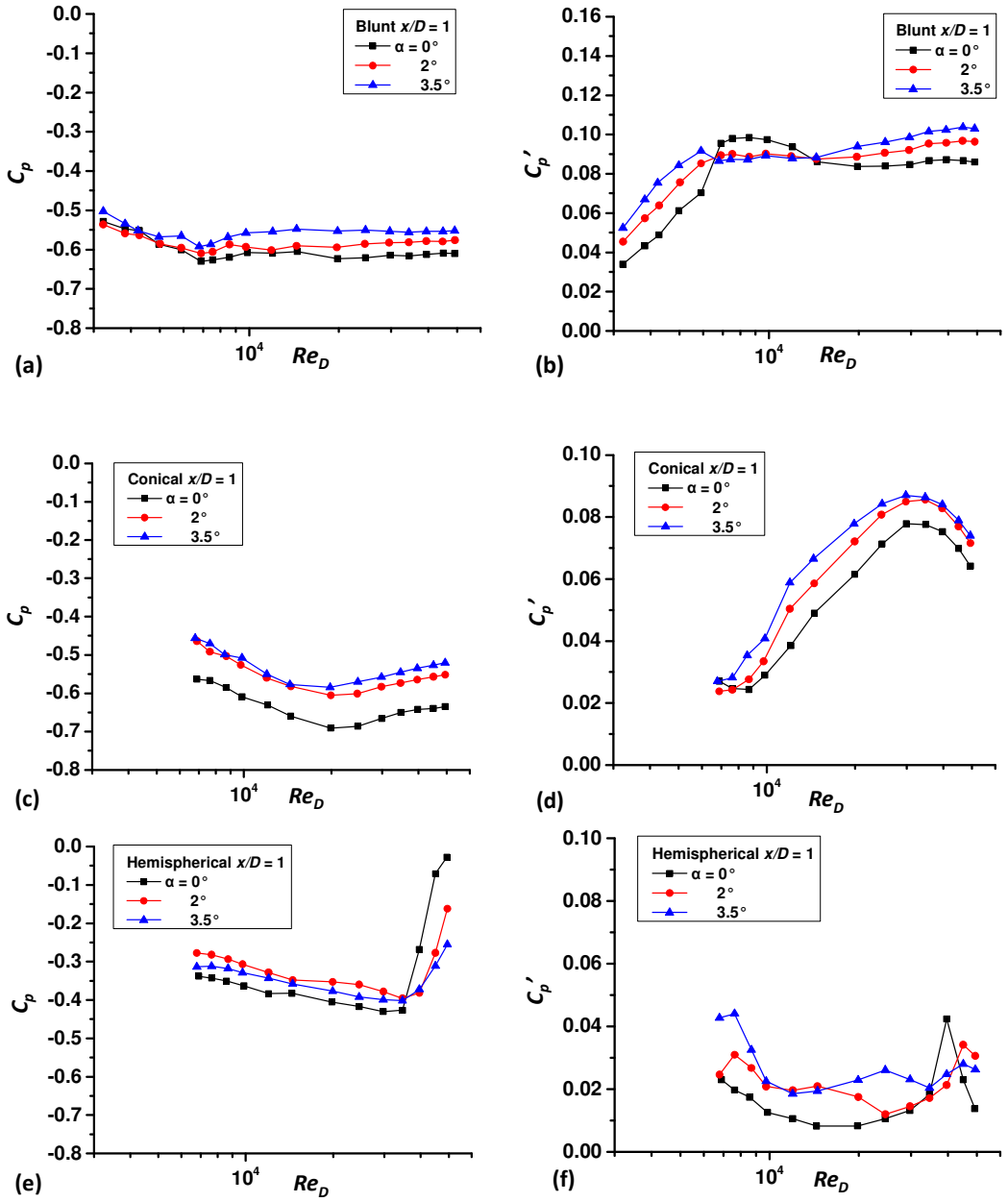


**Fig. 4.** Yaw angle effect on $C_p$ and $C_P^{'}$ for (a, b) blunt nose, (c, d) conical nose, (e, f) hemispherical nose.

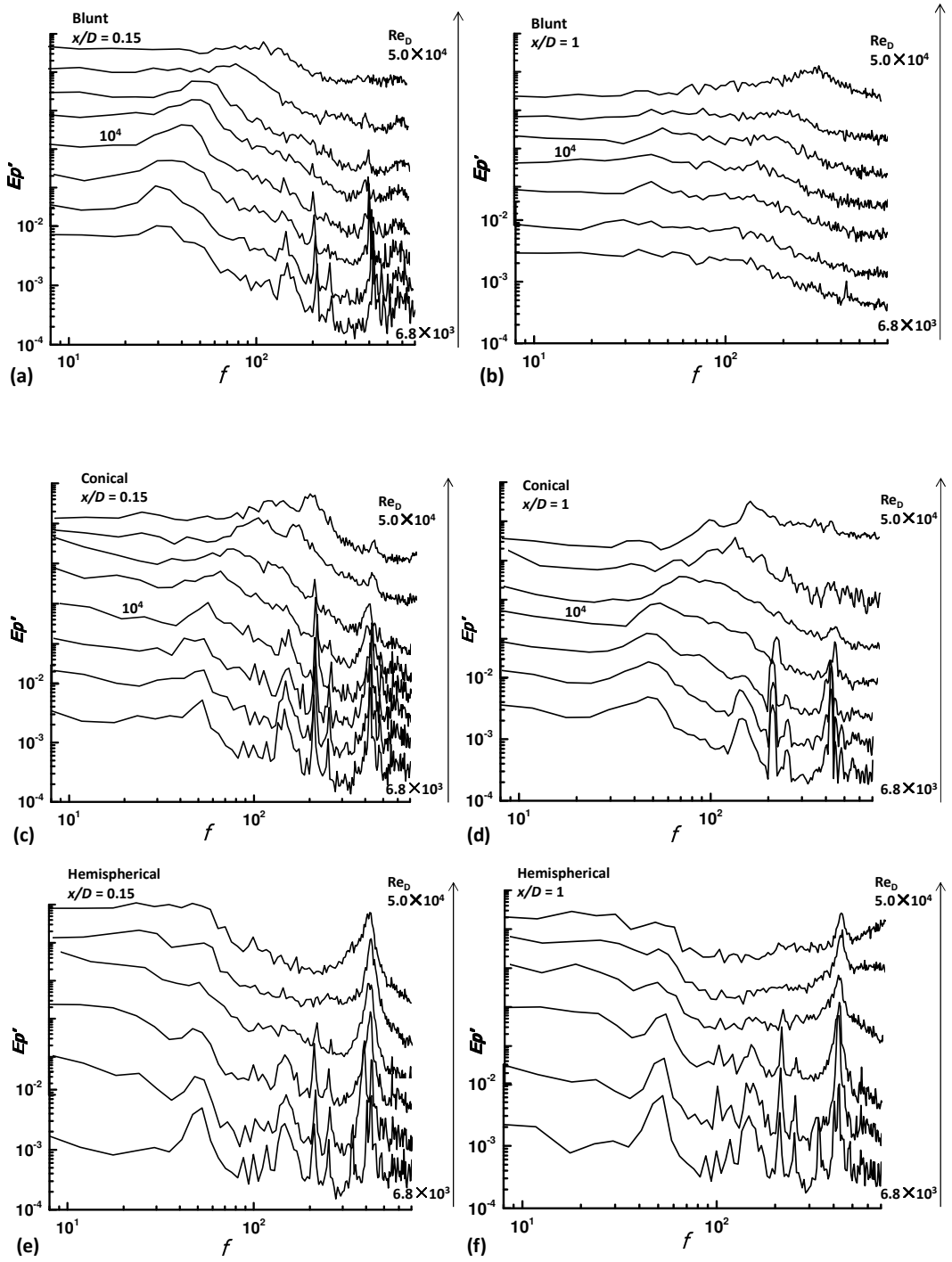


**Fig. 5.** Power spectral density functions $E_P$' of fluctuating pressure for three nose shapes at α = 0° **,** (a, c, e) *x/D* = 0.15 and (b, d, f) *x/D* = 1.0.

Figure 4 compares the yaw angle effect on $C_p$ and $C_P^{'}$ for the three nose shapes. With increasing α from 0° to 3.5°, $C_p$ magnitude reduces and $C_P^{'}$ is enhanced for both blunt and conical noses, while the magnitudes of $C_p$ and $C_P^{'}$ for the hemispherical nose are small and variations with α are irregular. Flow around the cylinder at α ≠ 0° is highly three-dimensional and asymmetric around the cylinder axis, while that at α = 0° is symmetric. The normal component of the flow at α ≠ 0° weakens the cavity intensity, resulting in $C_p$ declining for both blunt and

conical noses. With increasing α, the bubble is elongated accordingly and the normal component makes an additional contribution to $C_P^{'}$. On the other hand, both separation and reattachment points change with α for hemispherical nose, leading to an irregular change in $C_p$ and $C_P^{'}$. Again $C_p$ recovery and peak in $C_P^{'}$ are observed for $\alpha \neq 0°$ as well, but at higher $Re_D$.

Figure 5 illustrates power spectral density functions $E_{P'}$ of fluctuating pressure for the three noses at $x/D = 0.15$ and 1.0. There are two frequencies that are worthy to be discussed. One is a low frequency, $f \approx 35$ ~ 90 Hz (Fig. 5a), and the other is a high frequency, $f \approx 120$ ~ 300 Hz (Fig. 5b), both increase with $Re_D$. The low frequency results from the flapping motion of the separated shear layer, and the other is associated with the shedding of the large-scale eddies from the separation region [2]. The low frequency is however about $f = 50$ ~ 180 and 55 ~ 60 Hz for the conical and hemispherical noses, respectively, being less sensitive to $Re_D$ for the latter case. The high frequency is not discernible for the conical and hemispherical noses, perhaps because they are much less bluff than the blunt one.

## 4. Conclusions

$C_p$, $C_P^{'}$ and power spectral density function of fluctuating pressure are examined for a cylinder with three nose shapes, namely, blunt, cone and hemisphere in a wide range of $Re_D = 3.3\times10^3$ ~ $5\times10^4$. Measurements were conducted at three points on the cylinder, immediately behind the boundary-layer separation, in the separation bubble and behind the shear-layer reattachment. $C_p$ behind the reattachment was found to be smaller in magnitude compared to the other points measured. For the blunt cylinder, at $Re_D = 3.3\times10^3$ ~ $10^4$, the changing bubble size plays a significant role in determining both $C_p$ and $C_P^{'}$ in the separation bubble. Beyond the $Re_D$ range, $C_p$ and $C_P^{'}$ in the separation bubble was less sensitive to $Re_D$ because of the nearly unchanged bubble size. The magnitude of $C_p$ is smaller for the hemispherical nose and larger for the conical nose compared to that for the blunt nose. Furthermore $C_p$ and $C_P^{'}$ are highly sensitive to $Re_D$ for the hemispherical nose, as a result of easy shift of the separation point with increasing $Re_D$. The blunt nose presents highest $C_P^{'}$, while the hemispherical nose corresponds to the lowest $C_P^{'}$. With increasing α from 0° to 3.5°, $C_p$ declines and $C_P^{'}$ increases for both blunt and conical cases, while those for hemispherical case vary less regularly. The FFT analysis results of fluctuating pressure indicate that both low and high frequencies appear for the blunt nose, augmenting with the increasing $Re_D$. On the other hand, only the low frequency emerges for the conical and hemisphere noses.

## 5. Acknowledgement

Alam wishes to acknowledge supports given to him from Shenzhen Government through grant CB24405004 and from China Govt through '1000-young-talent-program'.

## 6. References

[1] T. Ota, "An Axisymmetric Separated and Reattached Flow on a Longitudinal Blunt Circular Cylinder", Journal of Applied Mechanics, pp. 311-315, 1975.

[2] M. Kiya, O. Mochizuki, H. Tamura, T. Nozawa, R. Ishikawa, and K. Kushioka, "Turbulence Properties of an Axisymmetric Separation-and-Reattaching Flow", AIAA Journal, Vol. 29, No. 6, pp. 936-941, 1991.

[3] Y.F. Dong, Z.L. Wei, C. Xu, X.Q. Jiang, and Y.F. Liao, "on Separated Shear Layer of Blunt Circular Cylinder", Acta Mechanica Sinica, Vol. 13, No. 4, pp. 313-322, 1997.

[4] H. Higuchi, H.Sawada, van Langen, and Pieter, "Flow over a Magnetically Suspended Cylinder in an Axial Free Stream", AIAA Paper 05-1078, 2005.

[5] H. Higuchi, van Langen, H.Sawada, and C.E. Tinney, "Axial Flow over a Blunt Circular Cylinder with and without Shear Layer Reattachment", Journal of Fluids and Structures, Vol. 22, pp. 949-959, 2006.

[6] H. Higuchi, H.Sawada, and H. Kato, "Sting-Free Measurements on a Magnetically Supported right Circular Cylinder aligned with the Free Stream", Journal of Fluid Mechanics, Vol. 596, pp. 49–72, 2008.

[7] T. Ota, and H. Motegi, "Turbulence Measurements in an Axisymmetric Separated and Reattached Flow over a Longitudinal Blunt Circular Cylinder", Journal of Applied Mechanics, Vol. 47, pp. 1-6, 1980.

[8] Z.J. Taylor, E. Palombi, R. Gurka, and G.A. Kopp, "Features of the turbulent flow around symmetric elongated bluff bodies", Journal of Fluids and Structures, Vol. 27, pp. 250-265, 2011.